



Original article

Synergistic approach to combating triple-negative breast cancer: DDR1-targeted antibody-drug conjugate combined with pembrolizumab

Shoubing Zhou ^{a, b}, Wenyu Li ^{a, b}, Dan Zhao ^c, Qijun Zhang ^{a, b}, Hu Liu ^{a, b, ***},
Tengchuan Jin ^{c, d, e, **}, Yueyin Pan ^{a, b, *}

^a Department of Breast Oncology, The First Affiliated Hospital of University of Science and Technology of China, Division of Life Sciences and Medicine, University of Science and Technology of China, Hefei, Anhui, 230031, China

^b Department of Breast Oncology, Anhui Provincial Cancer Hospital, Hefei, Anhui, 230031, China

^c Laboratory of Structural Immunology, The Chinese Academy of Sciences Key Laboratory of Innate Immunity and Chronic Disease, School of Basic Medical Sciences, Division of Life Sciences and Medicine, University of Science and Technology of China, Hefei, 230027, China

^d Department of Obstetrics and Gynecology, The First Affiliated Hospital of University of Science and Technology of China, Division of Life Sciences and Medicine, Center for Advanced Interdisciplinary Science and Biomedicine of International Health and Medicine (IHM), University of Science and Technology of China, Hefei, 230001, China

^e Institute of Health and Medicine, Hefei Comprehensive National Science Center, Hefei, 230027, China



ARTICLE INFO

Article history:

Received 15 June 2024

Received in revised form

23 August 2024

Accepted 10 September 2024

Available online 13 September 2024

Keywords:

Antibody-drug conjugates

Discoidin domain receptor 1

Triple negative breast cancer

Targeted therapy

Immunotherapy

ABSTRACT

Discoidin domain receptor 1 (DDR1) is overexpressed in various tumors, such as triple-negative breast cancer (TNBC), and is rarely expressed in normal tissues. These characteristics make DDR1 a preferable target candidate for the construction of an antibody-drug conjugate (ADC) for targeted therapy. Here, we investigated the preparation and preclinical efficacy of DDR1-DX8951, an ADC that includes an anti-DDR1 monoclonal antibody conjugated to DX8951 by a cleavable Gly-Gly-Phe-Gly (GGFG) linker. The anti-DDR1 monoclonal antibody was coupled to DX8951 (i.e., DDR1-DX8951), producing the targeted therapy ADC. The antitumor activities of DDR1-DX8951 monotherapy or DDR1-DX8951 plus pembrolizumab were assessed in TNBC mouse models. DDR1-DX8951 can specifically target DDR1, be quickly internalized by TNBC cells, and reduce the viability of TNBC cells *in vitro*. The potent antitumor activity of DDR1-DX8951 was revealed in TNBC xenograft models. Importantly, our investigation demonstrated that DDR1-DX8951 plus pembrolizumab not only revealed the inhibitory efficacy on tumor growth and metastasis but also played an important role in improving the immunosuppressive tumor microenvironment (TME) of TNBC. Taken together, this investigation provides justification for large-sample studies to further assess the safety and efficacy of DDR1-DX8951 plus pembrolizumab for TNBC clinical trials.

© 2024 The Author(s). Published by Elsevier B.V. on behalf of Xi'an Jiaotong University. This is an open access article under the CC BY-NC-ND license (<http://creativecommons.org/licenses/by-nc-nd/4.0/>).

1. Introduction

Triple-negative breast cancer (TNBC) is an aggressive subtype of breast cancer which is insensitive to established therapy regimes and related to poor prognosis. Patients with TNBC have the highest risk of relapse and metastasis among those with breast cancer [1]. Chemotherapy is still the cornerstone treatment for TNBC patients;

nevertheless, most patients experience relapse and metastasis after the first stage of treatment [2]. Treatment regimens for TNBC patients have been further optimized in recent years. Olaparib [3] and niraparib [4] are recommended by the National Comprehensive Cancer Network (USA) for the treatment of locally advanced/metastatic TNBC harboring germline breast cancer gene variations. Sacituzumab govitecan, an antibody-drug conjugate (ADC) that targets

Peer review under responsibility of Xi'an Jiaotong University.

* Corresponding author. Department of Breast Oncology, The First Affiliated Hospital of University of Science and Technology of China, Division of Life Sciences and Medicine, University of Science and Technology of China, Hefei, 230031, China.

** Corresponding author. Laboratory of Structural Immunology, the Chinese Academy of Sciences Key Laboratory of Innate Immunity and Chronic Disease, School of Basic Medical Sciences, Division of Life Sciences and Medicine, University of Science and Technology of China, Hefei, 230027, China.

*** Corresponding author. Department of Breast Oncology, The First Affiliated Hospital of University of Science and Technology of China, Division of Life Sciences and Medicine, University of Science and Technology of China, Hefei, 230031, China.

E-mail addresses: panyueyin@ustc.edu.cn (Y. Pan), jint@ustc.edu.com (T. Jin), drliuhu@ustc.edu.cn (H. Liu).

<https://doi.org/10.1016/j.jpha.2024.101100>

2095-1779/© 2024 The Author(s). Published by Elsevier B.V. on behalf of Xi'an Jiaotong University. This is an open access article under the CC BY-NC-ND license (<http://creativecommons.org/licenses/by-nc-nd/4.0/>).

the trophoblast cell surface antigen 2 molecule, is recommended for metastatic TNBC patients who have received two or more lines of therapy [5]. However, immunotherapy does not provide a clear clinical benefit to advanced/metastatic TNBC patients. The unsatisfactory efficacy of these agents may be attributable to the tumor microenvironment (TME) of TNBC, which is composed of desmoplastic stroma [6]. Such a TME represents a biological barrier that prevents T lymphocytes from effectively permeating tumor tissue and directly transferring signals, resulting in adverse outcomes [7,8]. Therefore, there is an urgent need to develop novel targets or therapeutics that can improve the immunosuppressive TME of TNBC while maintaining strong antitumor activity.

ADCs have emerged as a novel category of targeted therapy that has been shown to provide significant clinical benefit for many patients with various solid tumors, such as colorectal cancer [9], breast cancer [10,11], ovarian cancer [12,13], sarcoma [14], and non-small cell lung cancer [15,16]. In contrast to traditional molecular targeting and chemical methods, ADCs use peptide linkers to conjugate small-molecule agents to tumor-specific antibodies that can specifically target tumors while preventing them from accessing normal tissues. ADCs recognize specific cell membrane antigens and are subsequently internalized in a receptor-mediated manner, after which they release cytotoxic agents at the target site [17]. Compared with nanomedicines, ADCs feature superior target specificity and tissue permeability, providing a promising opportunity to enhance therapeutic agent delivery into cancer cells.

One important obstacle in constructing a TNBC-targeted ADC system is identifying potential targets that can be used to specifically distinguish between TNBC and normal cells. To improve the efficacy and safety of ADCs, ideal targets should be aberrantly expressed transmembrane receptors of TNBC cells that are negligibly expressed in nontumor cells, promoting the specific tumor accessibility of the ADCs. These properties of ADCs are essential for promoting the rapid and powerful endocytosis of effective payloads. Several traditional tumor adhesion molecules (e.g., intercellular adhesion molecule-1, trophoblast cell surface antigen 2, and epidermal growth factor receptor) have been recommended as targets in the treatment of TNBC [18,19]; however, the expression levels of cell surface receptors have not been confirmed quantitatively or comprehensively. We hypothesized that implementing quantitative screening of transmembrane receptors might result in the identification of optimal TNBC targets and target ADCs.

Discoidin domain receptor 1 (DDR1) is a member of the transmembrane receptor tyrosine kinase family [20]. DDR1 is aberrantly overexpressed in different tumor types (e.g., non-small cell lung, hepatocellular, pancreatic, colorectal, and breast cancer) and is closely associated with invasive behavior and poor prognosis [21–25]. In contrast to other receptors, DDR1 is activated via collagen fibres, which have been confirmed to constitute the main component of the extracellular matrix in several types of cancer [26,27]. Previous studies demonstrated that DDR1 impedes the infiltration of CD8⁺ T cells into tumor tissue, while the targeted binding of DDR1 antibodies to the DDR1 extracellular domain results in collagen fibre rearrangement, promoting CD8⁺ T-cell migration [7,28] (Scheme 1). A clinical trial of DDR1 humanized monoclonal antibodies has been initiated in advanced solid tumor patients and is currently ongoing (Trial No.: NCT05753722) [29]. In addition, exatecan has been known for nearly three decades and still has not been approved for clinical use, which may be attributed to its serious side effects [30,31]. The method of coupling exatecan with antibodies may improve the efficacy and reduce the side effects. Therefore, we hypothesized that DDR1-targeted ADCs could improve the immunosuppressive TME of TNBC while providing potent antitumor efficacy. Furthermore, groundbreaking progress has been made with immune checkpoint inhibitors in the field of tumor immunotherapy [8,32,33]. Blocking the inhibitory programmed cell death protein-1 (PD-1)/programmed

cell death protein ligand-1 (PD-L1) pathway induces strong T-cell responses and prevents tumor growth [34]. The KEYNOTE-355 study revealed that advanced/metastatic TNBC patients can benefit from combination treatment with pembrolizumab, and pembrolizumab is recommended for use in combination treatments for advanced/metastatic TNBC according to the National Comprehensive Cancer Network (USA) breast cancer guidelines [35]. Therefore, DDR1-targeted ADCs in combination with pembrolizumab could have synergistic antitumor effects on TNBC. To verify our hypothesis, we completed a proof-of-principle study in which DDR1-DX8951 was combined with pembrolizumab, which potently and persistently suppressed TNBC tumors *in vivo*.

2. Materials and methods

2.1. Materials

DDR1 rabbit monoclonal antibodies were purchased from Cell Signaling Technology, Inc. (Boston, MA, USA). Maleimidocaproyl (Mc)-Gly-Gly-Phe-Gly (GGFG)-DX8951, valine-citrulline (Vc)-monomethyl auristatin E (MMAE), and Mc-monomethyl auristatin F (MMAF) were purchased from MedChemExpress (Shanghai, China). The IgG rabbit monoclonal antibodies were provided by Abcam (Cambridge, UK), and used directly. Cyanine5.5 maleimide (Cy5.5) was purchased from Life-Cell (Shanghai, China). Pembrolizumab was obtained from MSD Corporation (Kennyworth, NJ, USA), and used directly. Human TNBC cell lines (SUM159, MDA-MB-231, Hs578T, and BT-549), a mouse TNBC cell line (E0771), and human mammary epithelial MCF10A cells were purchased from American Type Culture Collection (ATCC; Manassas, VA, USA). The characteristics of each cell line were validated via short tandem repeat polymorphisms. All the cell lines were also confirmed to be mycoplasma-free and continuously cultured within 15 passages.

2.2. Quantification of DDR1 expression

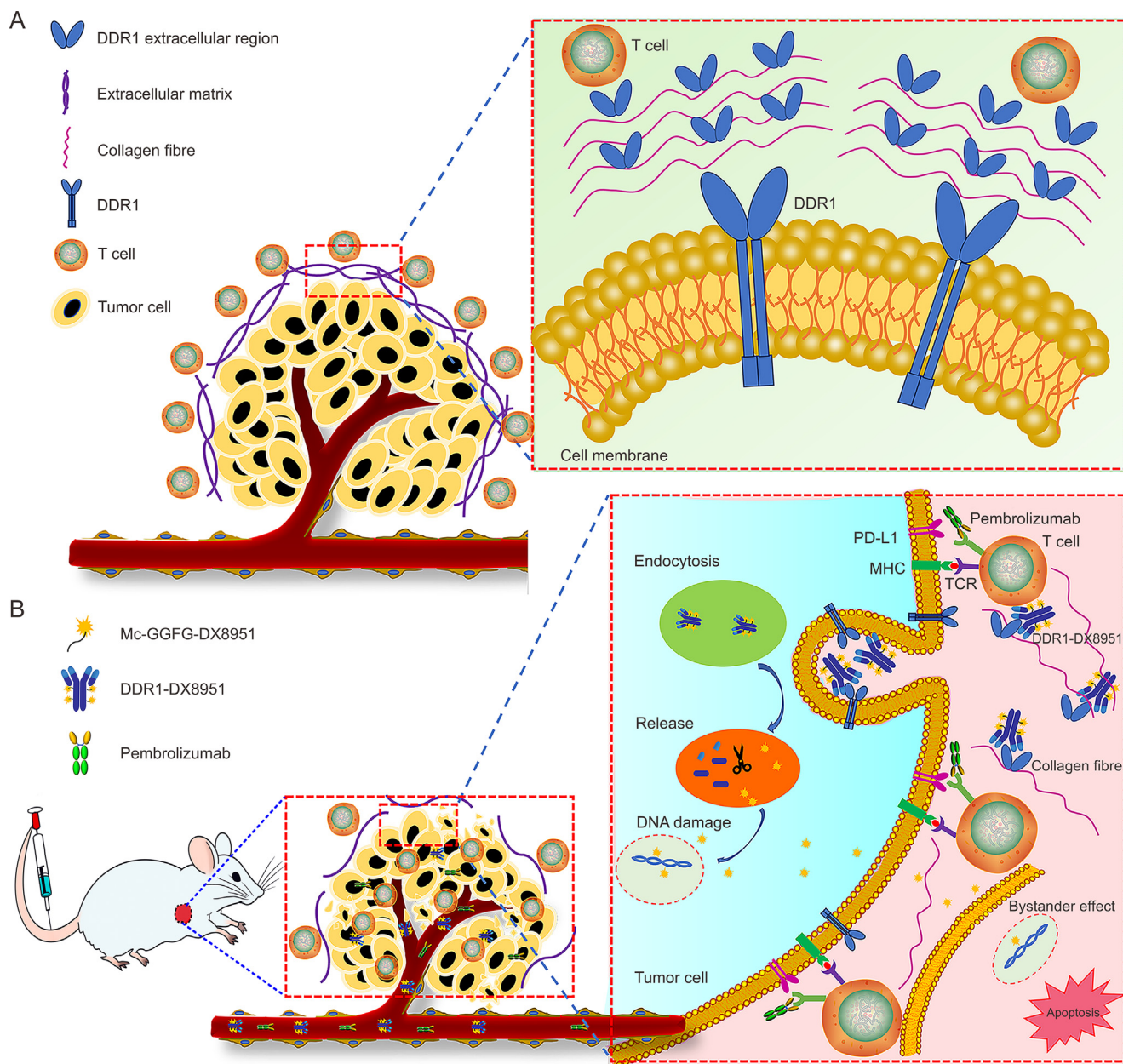
DDR1 expression in human TNBC cells, mouse TNBC cells, and MCF10A cells was assessed via flow cytometry as previously described [36]. The protein was quantified using quantum simple cellular microbeads. In brief, 10⁶ cells were obtained per experiment and rinsed three times using a rotating cycle method. The cells were sealed on ice using 1% bovine serum albumin (BSA), incubated with Cy5.5-conjugated antibodies at room temperature for 2 h, washed with phosphate-buffered solution (PBS) containing 1% fetal bovine serum (FBS) four times, and analyzed using flow cytometry.

2.3. Western blotting

DDR1 expression levels in different cell lines was also evaluated using the Western blotting as previously described [37]. Briefly, to extract total protein, 2 × 10⁶ cells were lysed in radioimmune precipitation assay (RIPA) buffer containing protease inhibitors. Subsequently, approximately 35–40 μg of total protein per sample was separated by sodium dodecyl sulfate-polyacrylamide gel electrophoresis (SDS-PAGE) and transferred onto nitrocellulose membrane. Blots were blocked with 5% nonfat milk in Tris-buffered saline with Tween (TBS-T) at room temperature for 1 h followed by primary antibody incubation overnight. Anti-DDR1 and anti-glyceraldehyde-3-phosphate dehydrogenase (GAPDH) antibodies were used as primary antibodies (1:400–1:2000 dilution). Blots were scanned with an Image Quant LAS 4000 from GE Healthcare Life Sciences (Beijing, China).

2.4. Immunofluorescence (IF) assay

The specificity of the DDR1 antibody in targeting TNBC cells was evaluated *in vitro* using IF. The IgG-Cy5.5 antibody was used as the



Scheme 1. Schematic illustration of discoidin domain receptor 1 (DDR1)-targeted antibody-drug conjugate (ADC) combined with pembrolizumab for concurrent immunotherapy and targeted therapy. (A) The binding of DDR1 extracellular region to collagen enforces aligned collagen fibres and obstructs T cell infiltration. (B) DDR1-DX8951 disrupt collagen fibre alignment, promote the intra-tumoral penetration of T cells, and improve drug targeted delivery, and the combination of DDR1-DX8951 and pembrolizumab enhance the synergistic antitumor activity. Mc: maleimidocaproyl; GGFG: Gly-Gly-Phe-Gly; PD-L1: programmed cell death protein ligand-1; MHC: major histocompatibility complex; TCR: T cell receptor.

control. The cells were cultured in eight-well plates at the appropriate density. After 24 h, the medium was replaced with medium containing the DDR1-Cy5.5 antibody, and the cells were incubated for an additional 4 h at 37 °C. The cells were then resuspended in ice-cold PBS and fixed in 4% paraformaldehyde. Paraffin-embedded sections of mouse tumors were rinsed twice with PBS. The following primary antibodies were used: anti-CD4 (1:100; HUABIO, Hangzhou, China) and anti-CD8 (1:50; HUABIO). The secondary antibodies fluorescein isothiocyanate (FITC)-tyramide (FITC-conjugated goat anti-rabbit IgG; Zhongshan Jinqiao Biotechnology Co., Ltd., Beijing, China) and Cy3-tyramide (Cy3-conjugated goat anti-rabbit IgG; Zhongshan Jinqiao Biotechnology Co., Ltd.) were used. The nuclei were counterstained using 4,6'-diamidino-2-phenylindole (DAPI) hydrochloride

containing anti-fluorescence quenching sealing liquid to contrast and locate the cells. Images were obtained via a Leica confocal microscope (Leica, Weztlar, Germany).

2.5. Immunohistochemistry (IHC) staining

Fresh tissue is fixed with 4% paraformaldehyde and paraffin-embedded sections were baked at 64 °C for 2 h, deparaffinized in xylene, and rehydrated in a series of ethanol solutions with decreasing concentrations. For antigen retrieval, sections were boiled in a constant volume and concentration of antigen repair solution for 12 min and then cooled at room temperature. Endogenous peroxidases were blocked with 3% H₂O₂. The samples were

incubated with the following primary antibodies overnight at 4 °C according to the instructions of the reagent kit: DDR1 (1:500; Cell Signaling Technology, Inc.), Ki67 (1:100; HUABIO), CD31 (1:500; Servicebio, Wuhan, China), and terminal deoxynucleotidyl transferase dUTP nick-end labeling (TUNEL) (1:500; Servicebio). Diaminobenzidine (DAB) was used as a color reaction system. Quantification analyses were conducted using ImageJ software according to the percentage of positively stained cells.

70 human breast tumor samples were collected at the Anhui Province Cancer Hospital (Hefei, China). All patients consented to participate in this investigation, and informed consent was obtained. The investigations were conducted following the tenets of the Declaration of Helsinki. Ethical monitoring was approved by the Ethics Committee of the Anhui Province Cancer Hospital (Approval No.: 2022237). IHC investigations were performed on 50 human TNBC tissue samples (stage I, 15 cases; stage II, 15 cases; stage III, 10 cases; and stage IV, 10 cases) and 20 normal mammary tissue samples to determine DDR1 expression as previously described [38]. IHC staining was scored by calculating H-scores in which the percent of cells staining strong (3+), moderate (2+), and weak (1+) were multiplied according to the formula: H-score = 3 × (percentage of cells staining 3+) + 2 × (percentage of cells staining 2+) + 1 × (percentage of cells staining 1+).

2.6. Enzyme-linked immunosorbent assay (ELISA)

Tumor-bearing mice blood were collected for detection of tumor necrosis factor- α (TNF- α), and interferon- γ (IFN- γ). The serum concentrations of interleukin 2 (IL-2), TNF- α , and IFN- γ were analyzed using ELISA kits (Elabscience, Wuhan, China) and experiment was carried out according to the manufacturer's protocol.

2.7. Flow cytometer

Flow cytometer was used to explore tumor cell counting and T cell counting in tissue. For culturing cells, cells were digested with trypsin followed by antibody marking. For tissue sample, the method for tumor tissue dissociation was as follows. First, the tumor tissue was crushed into small pieces of 1–3 mm in the centrifuge tube. Second, the tube was shaken on a constant temperature shaker for 1 h after adding collagenase solution. Next, the mixture was filtered using a filter (70 μ m) and collected cell suspension was centrifuged (400 g, 7min) for three times. Finally, single cells are recognized by the corresponding antibodies. Antibody used in this section of the experiment include anti-CD45-BV421 (Becton, Dickinson and Company, Franklin Lakes, NJ, USA), anti-CD4-FITC (Becton, Dickinson and Company), anti-CD3-allophycocyanin (APC) (Becton, Dickinson and Company), and anti-CD8-APC-Cy7 (Becton, Dickinson and Company). Flow cytometry data was obtained via a flow cytometer instrument (Beckman Coulter Life Sciences, Shanghai, China). The FlowJo software (version 10.8.1) was used to analyze the flow cytometry data.

2.8. Cell imaging studies

The cells were cultured in six-well plates at the appropriate density. The medium was completely replaced with medium mixed with DDR1-Cy5.5 antibody the next day, and the cells were incubated for an additional 4 h at 37 °C. Subsequently, the cells were resuspended in ice-cold PBS and assessed using an image stream X Mark II imaging flow cytometer (Merck Millipore, Seattle, WA, USA).

2.9. Preparation and synthesis of ADCs

The DDR1-DX8951 drug conjugate was generated as previously described [39]. DDR1 (500 μ L, 0.2 mg/mL) or IgG (500 μ L, 0.2 mg/

mL) antibody was added to sodium bicine buffer (200 μ L, 1 M, pH 8.0) and sodium diethylenetriaminepentaacetic acid (20 μ L, 100 Mm, pH 7.0). Subsequently, the reduction reaction was conducted using four equivalents of tris(carboxyethyl)phosphine (TCEP) for 2 h at 37 °C, and the obtained solution was subsequently mixed with four equivalents of maleimidocaproyl-GGFG-exatecan (Mc-GGFG-DX8951) or Mc-Cy5.5. After shaking for 2 h, the gel was separated by filtration (Sephadex G25, 1.0 g; Yuanye Bio-Technology Co., Ltd., Shanghai, China) and eluted with PBS. The reaction was monitored using a capillary high performance liquid chromatography (HPLC) (Ultimate 3000, Thermo Fisher Scientific Inc., Waltham, MA, USA)/electrospray quadrupole time-of-flight mass spectrometry (MS) system equipped with an ACQUITY UPLC Protein BEH C₄ column (300 Å, 1.7 μ m, 2.1 mm × 50 mm) (Waters, Milford, MA, USA). The elution schemes were as follows: water containing 0.1% (v/v) formic acid as mobile phase A; acetonitrile containing 0.1% (v/v) formic acid as mobile phase B; linear gradient: 5%–100% B, 10 min; 100%–100% B, 5 min; 100%–5% B, 2 min; and 5%–5% B, 2 min; and flow rate as 0.3 mL/min. The average drug to antibody ratio (DAR) values were obtained using liquid chromatography (LC)-MS analysis. Other ADCs in this study were constructed using similar methodologies.

2.10. In vitro cytotoxicity studies

TNBC cells were cultured in 96-well chamber slides at a density of 5 × 10³ cells/well. Medium was substituted with medium supplemented with epirubicin (EPI), IgG-DX8951, DDR1-DX8951, DDR1-MMAE, IgG-MMAE, DDR1-MMAF, or IgG-MMAF at various concentrations. After 72 h, cytotoxicity was evaluated using a Cell Counting Kit-8 (CCK-8) assay. In brief, the drug-containing medium was removed, and the cells were gently cleaned with ice-cold PBS before incubation with CCK-8 medium at 37 °C for 4 h. Cell proliferation inhibition was estimated by comparing the absorbance of cells treated with agents to that of blank cells.

2.11. Establishment of TNBC organoid cultures

TNBC organoid cultures were generated as follows. Tumor tissues were cut into small pieces and digested enzymatically in tumor tissue digestion solution for 30 min at 37 °C in a constant temperature shaking incubator. Single cells were collected after filtering the suspension through a 100- μ m mesh filter. Subsequently, cells embedded in Matrigel were seeded on 24-well culture dishes and complete growth medium was added. Complete medium was replaced every three days. Organoid passage was completed every two weeks.

Cytotoxicity studies in TNBC organoids was conducted according to the previously published protocol [40]. Organoids were treated with PBS, IgG-DX8951, EPI, or DDR1-DX8951 for three days, and cell viability was measured using the Cell Titer-Glo three-dimensional (3D) Cell Viability kit assay (Promega Corporation, Beijing, China).

2.12. In vivo biodistribution studies

Mouse tumorigenicity assays were performed following the principles approved by the Institutional Animal Care and Use Committee of the University of Science and Technology of China (2022-N(A)-143). The study protocol for human derived material was approved by the Institutional Review Board (IRB) of Anhui Province Cancer Hospital (Hefei, China) (Approval No.: 2022237) in accordance with the Declaration of Helsinki of the World Medical Association. Approximately 2 × 10⁶ TNBC cells (MDA-MB-231 or E0771) were subcutaneously injected into the right dorsal flank of

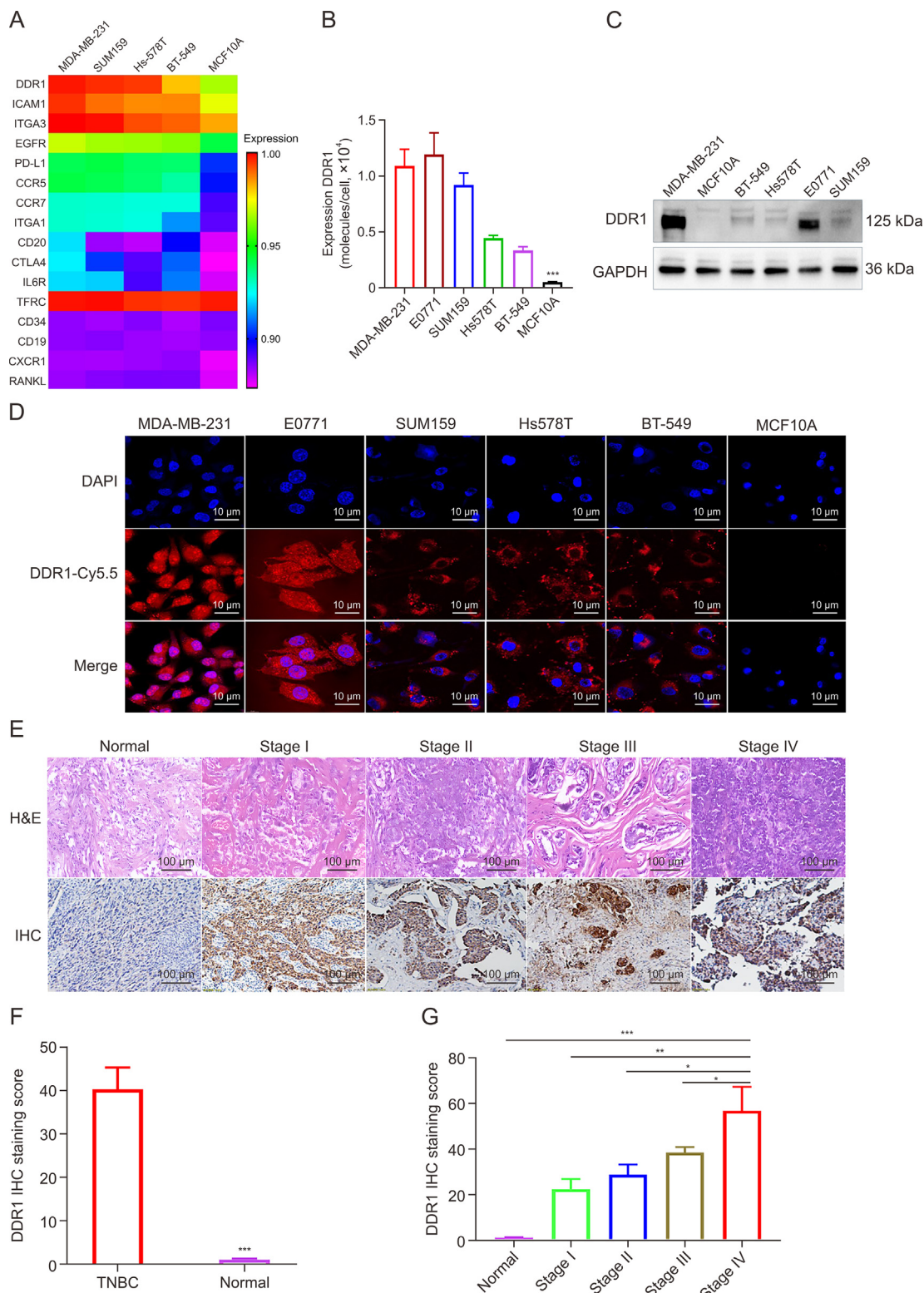
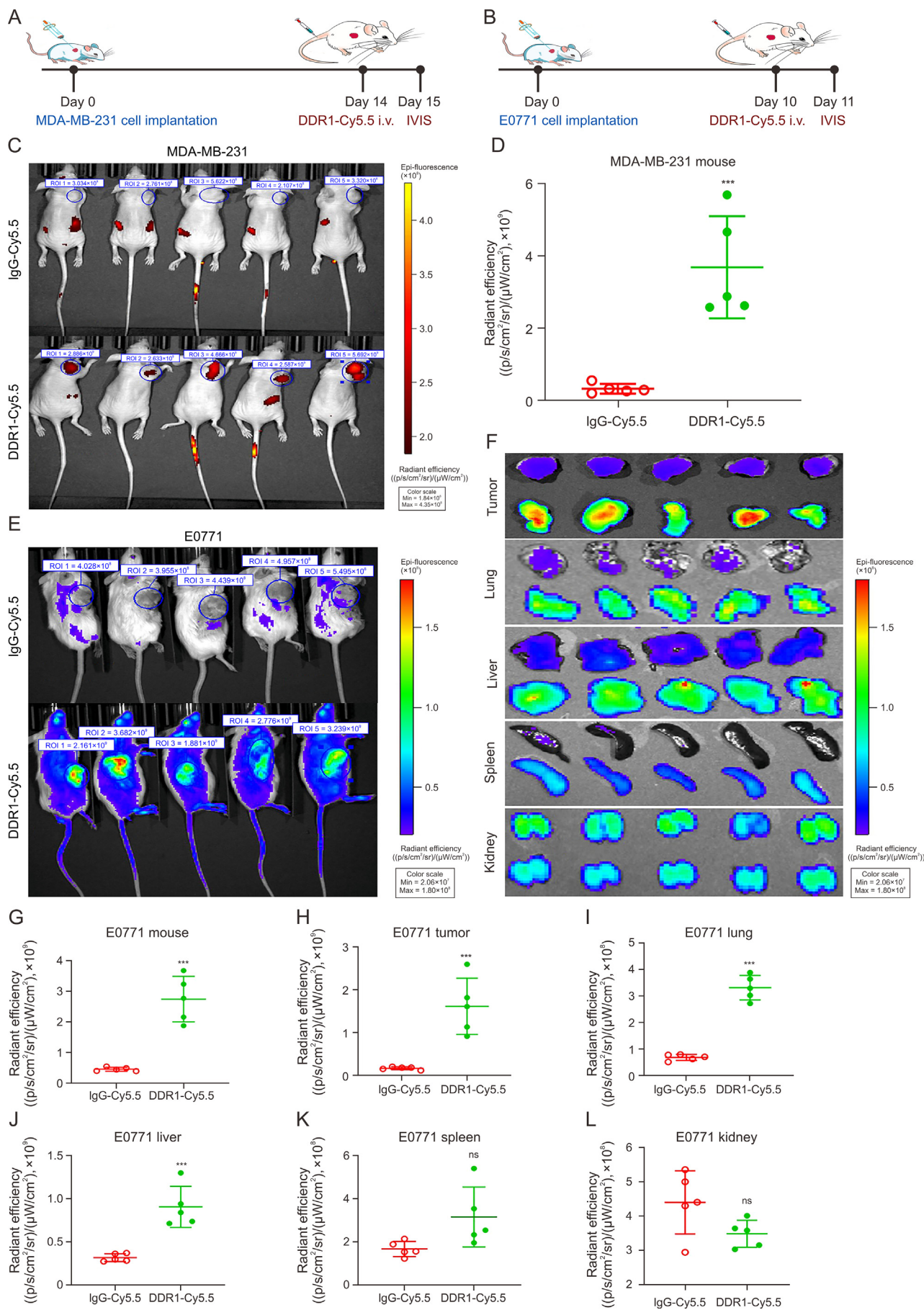


Fig. 1. Differential overexpression of discoidin domain receptor 1 (DDR1) in triple-negative breast cancer (TNBC) tissues and cells. (A) Heatmap of membrane proteins expression in TNBC cells, compared with normal human mammary epithelial cells. (B) Flow cytometry of DDR1 in TNBC cell lines. (C) Western blotting of DDR1 and glyceraldehyde-3-phosphate dehydrogenase (GAPDH) in TNBC cell lines. (D) Immunofluorescence (IF) staining of DDR1 in TNBC and normal human mammary epithelial cells. (E) Representative images of hematoxylin and eosin (H&E) and immunohistochemistry (IHC) stainings of DDR1 in human TNBC tumor tissues at different stages and normal human mammary tissues. (F) Comparison of DDR1 IHC staining score between TNBC and normal tissues. (G) Pathological scores for tumor correlated with tumor node metastasis (TNM) stages. **P* < 0.05, ***P* < 0.01, and ****P* < 0.001. DAPI: 4,6'-diamidino-2-phenylindole; Cy5.5: cyanine5.5 maleimide.



six-week-old female nude or BALB/c mice. After 1–2 weeks, the tumor volume reached 300 mm³. The mice were then randomly divided into different experimental groups ($n \geq 5$ per group) and injected with IgG-Cy5.5 or DDR1-Cy5.5 (5 mg/kg) via the tail vein. After 24 h, *in vivo* near-infrared (NIR) fluorescence was evaluated using an in-vehicle information system (IVIS) Lumina II system (PerkinElmer, Waltham, MA, USA). The fluorescence intensities of different tissues, including tumors, livers, lungs, kidneys, and spleens, were determined via IVIS.

2.13. *In vivo* treatment effects in TNBC mouse models

Peripheral blood mononuclear cells (PBMCs) were obtained from healthy human blood specimens using gradient centrifugation. PBMCs were incubated with Roswell Park Memorial Institute (RPMI) 1640 medium, the antibiotic antimycotic agent, and 1 mM pyruvate. PBMCs were cultured with T cell receptor (TCR) or IL-2 stimulation for three days.

For the *in vivo* antitumor activity assessments, TNBC cells (E0771 or MDA-MB-231) were inoculated into 6 to 8-week-old female BALB/c or NOD/ShiLjGptPrkdc^{em26}IL2rg^{em26}/Gpt (NSG) mice as described above [41]. When the tumor volume reached 100–150 mm³, the mice were randomly divided into groups, and 5×10^6 PBMCs were inoculated via the tail vein. Then, the BALB/c mice were treated with PBS, IgG-DX8951, EPI, or DDR1-DX8951 via tail vein injection. The NSG mice were injected with or without established concentrations of PBS, pembrolizumab, DDR1 antibody, DDR1-DX8951, or DDR1-DX8951 plus pembrolizumab. The tumor volume was determined using an electronic caliper twice to three times per week and calculated following the equation “tumor volume = length \times width²/2.” For the dose-dependency assessment, three incremental DDR1-DX8951 concentrations (1, 5, and 10 mg/kg) were tested in tumor-bearing mice (E0771). Subsequently, the tumor-bearing mice were anesthetized with CO₂, and blood was obtained by heart puncture. The blood was left to stand for 30 min; then the serum was obtained by centrifuging for 15 min at 2,000 g. The alanine aminotransferase (ALT), aspartate aminotransferase (AST), creatinine (Cre), and blood urea nitrogen (BUN) levels were assessed via ELISA kits from Huabangbio Co., Ltd. (Shanghai, China). Alterations in mouse body weight are negatively correlated with acute toxicity; thus, mouse body weight was carefully monitored, when the BALB/c mice were sacrificed and tumors were harvested. In addition, the expression levels of CD4, CD8, and TUNEL were evaluated in xenograft models.

The NSG mice were euthanized on day 42, and the tumors were harvested. Specimens were subjected to hematoxylin and eosin (H&E), DDR1, Ki67, and CD31 IHC, TUNEL IF, and CD4 and CD8 double IF stainings. Tumor tissues were pulverized to obtain single-cell suspensions for assessments of *in vivo* antitumor immunity and the efficacy of immunotherapy. Tumor-infiltrating lymphocytes were incubated with anti-CD45-BV421, anti-CD4-FITC, anti-CD3-APC, and anti-CD8-APC-Cy7 antibodies to evaluate CD8⁺ T cells. The cells collected were evaluated via flow cytometry. The serum levels of IL-2, TNF- α , and IFN- γ in NSG mice from each group were evaluated using ELISA kits.

2.14. *In vivo* antimetastasis assessment

The lungs and livers of each group of mice were prepared for imaging and histopathological analysis with H&E staining. The number of metastatic nodules was also determined to evaluate the antimetastatic efficacy of the assessed agents *in vivo*. The survival rates of tumor-bearing mice in the PBS and DDR1-DX8951 plus pembrolizumab groups were also monitored.

2.15. Statistical analysis

The data are presented as the mean \pm standard deviation (SD). Statistical analyses were conducted via GraphPad Prism (version 9) using a two-tailed Student's *t*-test or one-way analysis of variance (ANOVA). Survival analysis was conducted via the log-rank test. The significance levels are expressed as * $P < 0.05$, ** $P < 0.01$, and *** $P < 0.001$.

3. Results

3.1. Evaluation of TNBC targets

We used our platform to screen cell surface targets to identify a desirable target for discriminating between TNBC and normal cells (Fig. 1A). We first performed quantitative screening of a set of tumor-associated proteins in four established human TNBC cell lines (MDA-MB-231, BT-549, SUM159, and Hs578T) and one established mouse TNBC cell lines (E0771) compared with MCF10A as the control. DDR1 was overexpressed in TNBC cells but almost absent from human mammary epithelial MCF10A cells (Fig. 1B). Consistent results were obtained in the Western blotting experiment (Fig. 1C). We further confirmed the overexpression of DDR1 in TNBC cells via IF. DDR1 was significantly overexpressed on the plasma membrane of TNBC cell lines (MDA-MB-231, E0771, BT-549, SUM159, and Hs578T) but was not expressed in normal MCF10A cells (Fig. 1D). The overexpression of DDR1 in TNBC cells allows the easy evaluation of DDR1-targeting therapeutics.

To validate whether DDR1 expression is associated with TNBC tissues in clinical practice, we performed IHC staining of DDR1 in 50 human TNBC tumor tissue specimens and 20 mammary tissue specimens. As shown in Figs. 1E and F, DDR1 was strongly overexpressed on the plasma membrane of TNBC cells from tumors at different pathological stages but rarely expressed in normal mammary tissue specimens. The IHC results indicated that the expression level of DDR1 was positively correlated with the tumor node metastasis (TNM) stage (Fig. 1G).

3.2. Recognition and targeting of TNBC tumors by DDR1 antibodies

We assessed the targeting and biodistribution of DDR1-targeted ADCs using MDA-MB-231 tumor-bearing immunodeficient nude mouse xenograft models. E0771 tumor-bearing immunocompetent BALB/c mouse xenograft models were used to assess various immune microenvironments. DDR1 targeting was first evaluated in a human TNBC nude mouse model (Fig. 2A). We also assessed DDR1-Cy5.5 biodistribution in immunocompetent BALB/c mice (Fig. 2B).

Fig. 2. Specific recognition and biodistribution of discoidin domain receptor 1 (DDR1) antibody. (A) Schematic design of human triple-negative breast cancer (TNBC) biodistribution in an immunocompromised nude mouse model. (B) Schematic design of murine TNBC biodistribution in an immunocompetent BALB/c mouse model. (C) *In vivo* near infrared (NIR) fluorescence imaging of nude mice at 24 h after intravenous injection IgG-cyanine5.5 maleimide (Cy5.5) or DDR1-Cy5.5 ($n = 5$). (D) Corresponding quantification of fluorescence intensity in MDA-MB-231 tumors. (E) *In vivo* NIR fluorescence imaging of BALB/c mice at 24 h after intraous injection IgG-Cy5.5 or DDR1-Cy5.5 ($n = 5$). (F) *Ex vivo* NIR fluorescent images of E0771 tumors and four normal organs treated by IgG-Cy5.5 and DDR1-Cy5.5 ($n = 5$). (G–L) Quantified E0771 mice, tumor, and normal organ accumulation of IgG-Cy5.5 or DDR1-Cy5.5: fluorescence intensity analysis of tumor in mice (G), *ex vivo* tumor (H), lung (I), liver (J), spleen (K), and kidney (L). *** $P < 0.001$. ns: not significant. IVIS: in-vehicle information system; ROI: region of interest.

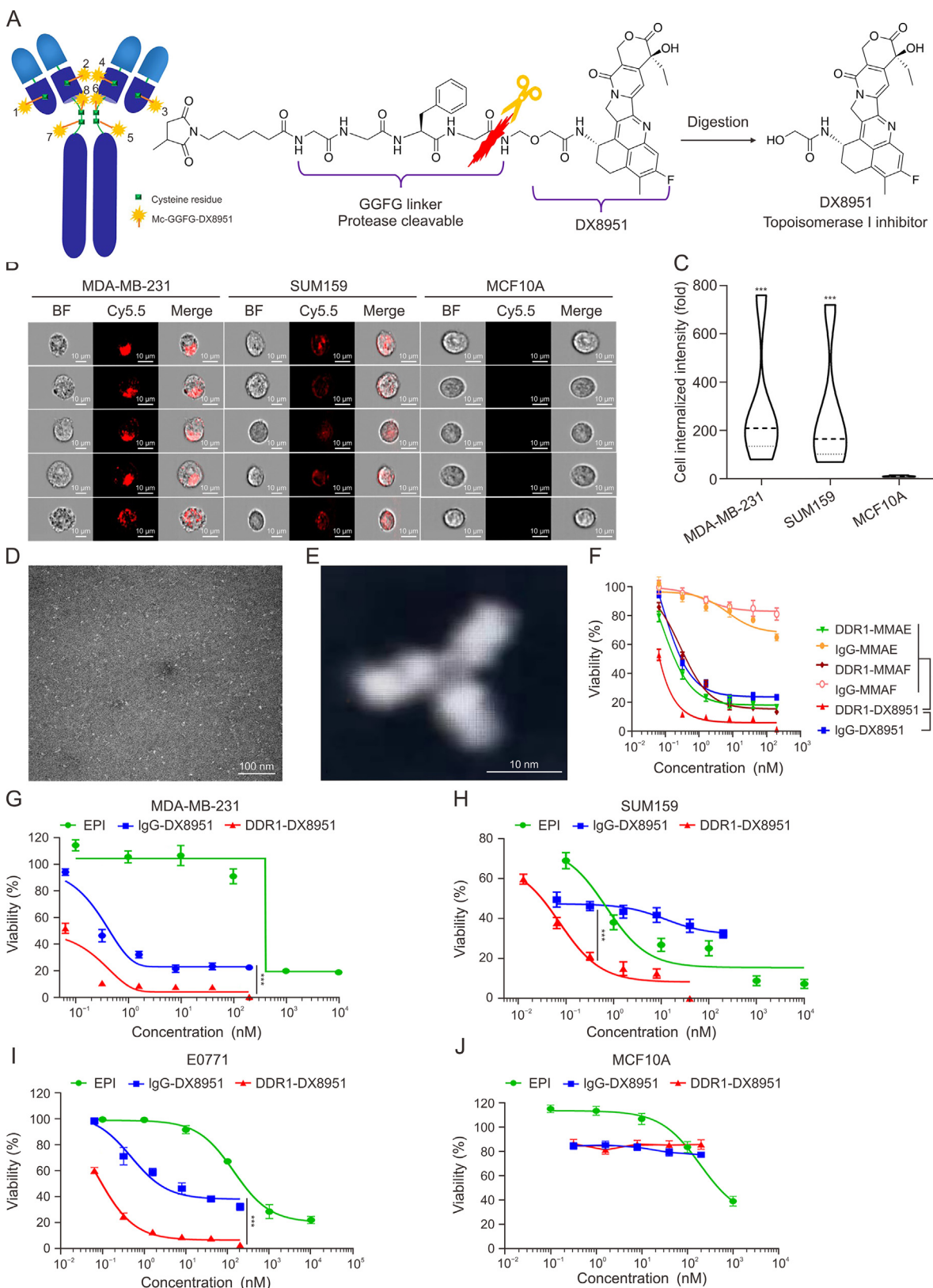


Fig. 3. Structure and discoidin domain receptor 1 (DDR1)-specific activity of DDR1-DX8951. (A) Schematic structure of DDR1-DX8951. 1–8 represents sites capable of conjugating drugs, respectively. (B) Representative imaging flow cytometry images showing the triple-negative breast cancer (TNBC)-specific internalization of DDR1 antibody in MDA-MB-231, SUM159, and MCF10A cells. (C) Signal intensity analysis for DDR1 antibody-mediated cell internalization ($n = 10,000$). (D) Transmission electron microscopy (TEM) images of DDR1-DX8951 negatively stained (white dots). (E) The true morphology of DDR1-DX8951 observed by TEM. (F) Screening of cytotoxic payload with different linker that conjugated to DDR1 antibody. (G–J) Cell viability assays to measure the antitumor activity of DDR1-DX8951 to MDA-MB-231 (G), SUM159 (H), E0771 (I), and MCF10A (J), compared with IgG-DX8951 and epirubicin (EPI). *** $P < 0.001$. Mc: maleimidocaproyl; GGFG: Gly-Gly-Phe-Gly; BF: bright field; Cy5.5: cyanine5.5 maleimide; MMAE: monomethyl auristatin E; MMAF: monomethyl auristatin F.

We covalently coupled DDR1 antibodies with Cy5.5 (DDR1-Cy5.5), a red fluorescent dye, and administered DDR1-Cy5.5 through the tail vein to MDA-MB-231 tumor-bearing mice at an equivalent dosage of 5 mg/kg (Fig. S1 and Table S1). Cy-5.5-labeled IgG monoclonal antibodies (IgG-Cy5.5) were used as a nontargeting control (Fig. S2 and Table S2). To determine the tumoral accumulation of DDR1-Cy5.5 antibodies, fluorescence intensities *in vivo* were measured using an IVIS® Spectrum scanner at 24 h post-injection. As shown in Fig. 2C, nude mice inoculated with DDR1-Cy5.5 exhibited significant intratumoral agglomeration, approximately 9-fold greater than that observed in the IgG-Cy5.5 group (Fig. 2D). Unlike the nontargeting IgG-Cy5.5, DDR1-Cy5.5 can target and selectively accumulate in tumor tissue. A perfect immune condition can potentially reflect the true interactions between DDR1 antibodies and the TME to a greater extent than the immunodeficient xenografted model. As shown in Fig. 2E, DDR1-Cy5.5 sustains the underlying mechanism of E0771 tumor targeting in BALB/c mice,

similar to the results obtained in nude mouse model. The bio-distribution of DDR1-Cy5.5 was also assessed in tumors and four major organs (Fig. 2F). Specific agglomeration of DDR1-Cy5.5 was explored in BALB/c mice and the detached tumor (Figs. 2G, 2H, and S3). Enhanced accumulation of DDR1-Cy5.5 was detected in the lung and liver (Figs. 2I and J), which was attributed to the rich blood flow and increased metabolism. No specific agglomeration of DDR1-Cy5.5 was detected in the spleen or kidney (Figs. 2K and L). These *in vivo* outcomes contributed to the preparation of DDR1-ADCs for TNBC-targeted treatment.

3.3. Design and characterization of DDR1-ADCs

Given that receptor-mediated endocytosis plays an important role in ADC development, we explored the receptor-mediated endocytosis of TNBC cells using an imaging flow cytometry experiment. The structural composition of DDR1-DX8951 is shown (Fig. 3A). DDR1-Cy5.5 was

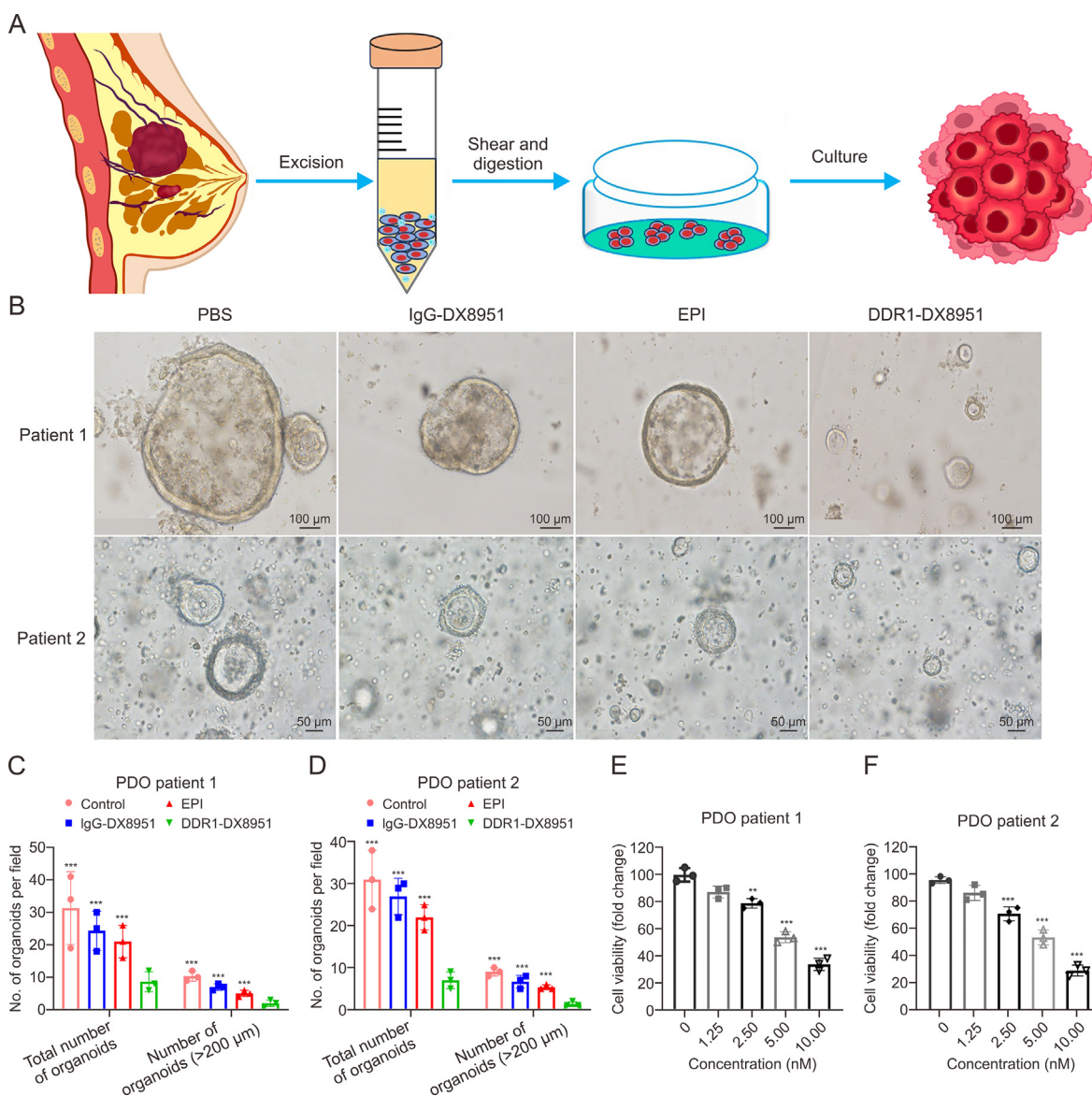
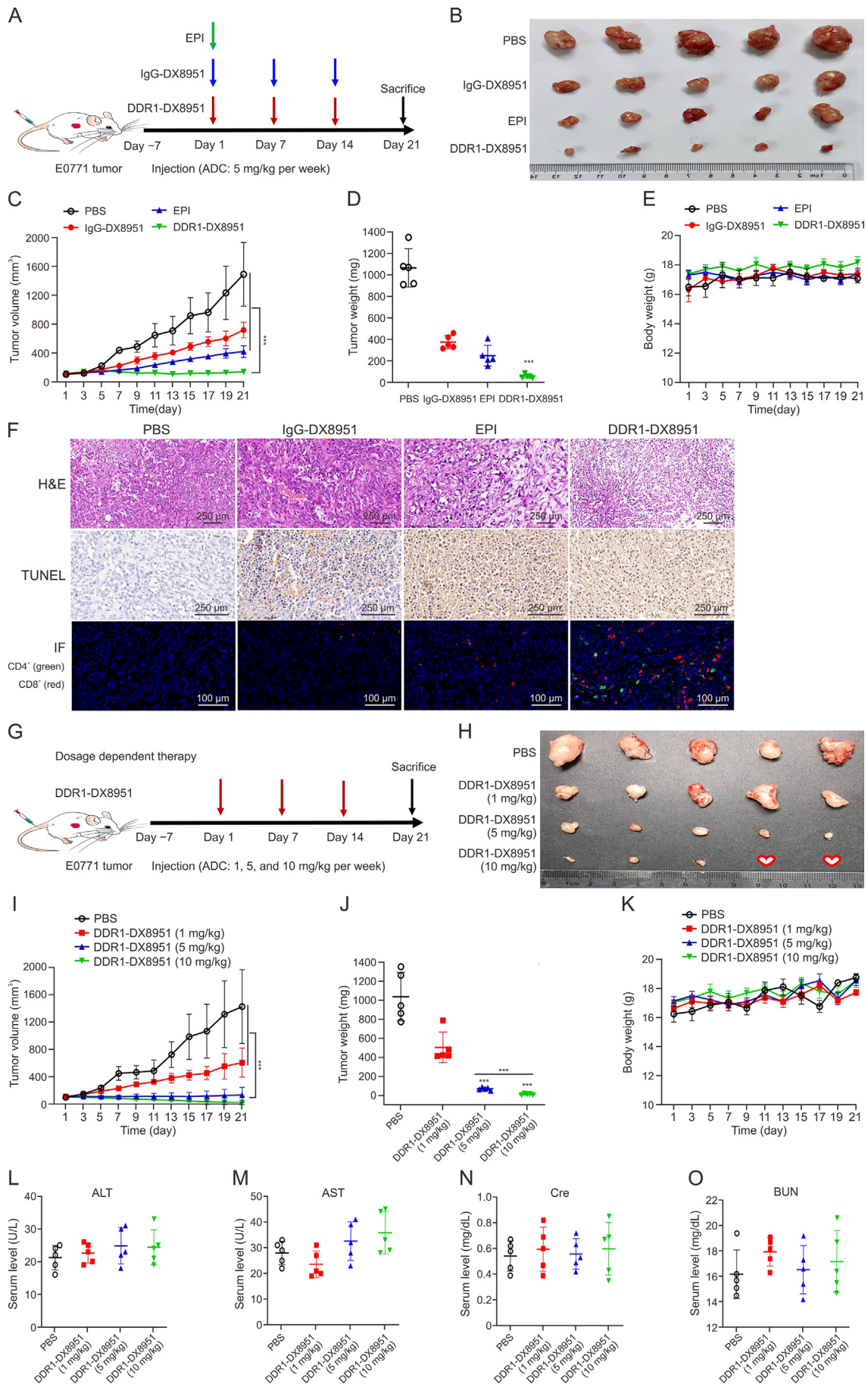


Fig. 4. Efficacy of discoidin domain receptor 1 (DDR1)-DX8951 in patient-derived organoid (PDO) models of triple-negative breast cancer (TNBC). (A) Schematic view of the TNBC PDO model. (B) Representative images of the patient 1 and patient 2 organoids in different treatment groups. (C, D) Statistics of TNBC organoid size and relative number of formed organoids for PDO patient 1 (C) and patient 2 (D). (E, F) The proliferation assay of TNBC PDO treated with vehicle and exponentially increasing concentrations of DDR1-DX8951 for 72 h in patient 1 (E) and patient 2 (F). ** $P < 0.01$ and *** $P < 0.001$. PBS: phosphate-buffered solution; EPI: epirubicin.



significantly internalized by both MDA-MB-231 and SUM159 cells by DDR1 receptor-mediated endocytosis, while DDR1-Cy5.5 was hardly observed within MCF10A cells due to the marked absence of DDR1 receptor expression (Fig. 3B). The fluorescence intensity of DDR1-Cy5.5 in human TNBC cells was approximately 200-fold greater than that in MCF10A cells (Fig. 3C). These results demonstrate that this DDR1 antibody may be a desirable TNBC tumor-targeting ligand. To validate the characterization of DDR1-ADC, the morphology and size of DDR1-DX8951 were measured using transmission electron microscopy (TEM). The TEM image demonstrated the “Y” morphology and approximately 18 nm of the size of DDR1-DX8951 (Figs. 3D and E). We constructed a promising DDR1-ADC as a proof-of-principle for DDR1-targeted TNBC treatment. Considering the correlation between the effective payload of the ADC and therapeutic efficacy, we initially explored the desired ADC formulation for targeted TNBC treatment through quantitative screening. We constructed several ADCs with different cytotoxic payloads (Vc-MMAE, Mc-GGFG-DX8951, and Mc-MMAF) at identical drug-to-antibody ratios and evaluated their cytotoxicity against MDA-MB-231 cells. DDR1-GGFG-DX8951 (DDR1-DX8951) had the lowest half-maximal drug inhibitory concentration (IC_{50}) (0.067×10^{-9} M) among the three validated ADCs (other IC_{50} values: 0.71×10^{-9} to 3.21×10^{-9} M) in MDA-MB-231 cells (Fig. 3F). Notably, the IC_{50} of DDR1-DX8951 was over 6500-fold lower than that of EPI (441.30×10^{-9} M) (Fig. 3G), the classical chemotherapeutic for TNBC. Mc-GGFG-DX8951 is a classical ADC formulation including the efficacious DNA topoisomerase I inhibitor DX8951. Therefore, we chose Mc-GGFG-DX8951 as our preferred component and prepared DDR1-DX8951, an excellent DDR1-ADC for TNBC-targeted treatment (Fig. S4). Furthermore, IgG-GGFG-DX8951 (IgG-DX8951) was tested as a nontargeting control using the same coupling method (Fig. S5). The DARs for DDR1-DX8951 and IgG-DX8951 were monitored via the feed ratio of Mc-GGFG-DX8951 to the other antibodies; 4.5 for DDR1-DX8951 and 4.8 for IgG-DX8951 were obtained, confirmed using LC-MS analysis (Tables S3 and S4).

3.4. Selective cytotoxicity of DDR1-DX8951 toward TNBC cells

The cytotoxicity of DDR1-DX8951 was evaluated in TNBC cell lines (MDA-MB-231, SUM159, and E0771) and MCF10A cells. The anthracycline antitumor drugs EPI and nontargeting IgG-DX8951 were used as controls. DDR1-DX8951 exhibited potent cytotoxicity against MDA-MB-231, SUM159, and E0771 cells (Figs. 3G–I). The IC_{50} values of DDR1-DX8951 were 0.067×10^{-9} M (MDA-MB-231 cells), 0.025×10^{-9} M (SUM159 cells), and 0.022×10^{-9} M (E0771); these values are significantly lower than those obtained with EPI and IgG-DX8951 (0.58×10^{-9} to 441.3×10^{-9} M). Furthermore, no cytotoxicity was detected in MCF10A cells treated with DDR1-DX8951 due to the absence of the DDR1 receptor (Fig. 3J). The outcomes of the cytotoxicity experiment strongly supported assessing the antitumor efficacy of DDR1-DX8951 in TNBC xenograft models.

3.5. Antitumor activity in TNBC organoids

We conducted a patient-derived organoid (PDO) model utilizing specimens of TNBC to further assess the antitumor activity of

DDR1-DX8951. The tumor cells from two TNBC patients were cultured in a 3D system to develop TNBC organoids (Figs. 4A and B). As shown in Figs. 4C and D, DDR1-DX8951 led to significant growth inhibition of TNBC organoids, manifested as a decrease in organoid size and number. The dose-dependent growth inhibition of TNBC PDO demonstrated the potent inhibitory effect of DDR1-DX8951 on TNBC progression (Figs. 4E and F), further confirming the potential antitumor effectiveness of DDR1-DX8951 in the treatment of TNBC organoids.

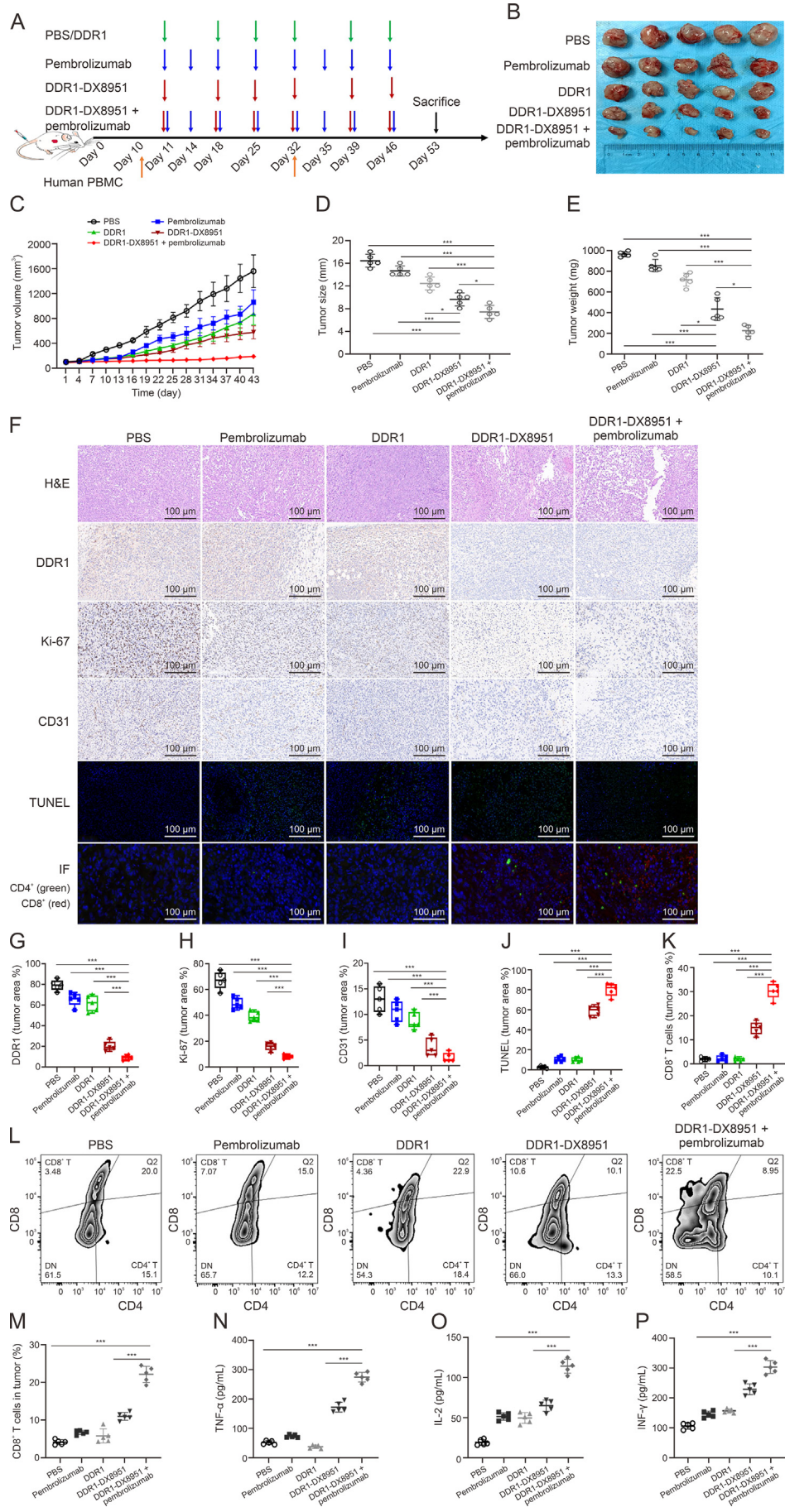
3.6. In vivo antitumor efficacy of DDR1-DX8951

We constructed several groups of orthotopic TNBC models to assess the efficacy of the potent DDR1-DX8951 ADC *in vivo*. We assessed the *in vivo* efficacy of DDR1-DX8951 in an orthotopic TNBC model (E0771) by applying DDR1-DX8951 (5 mg/kg) targeted therapy when the tumor size increased to approximately 100 mm^3 (Fig. 5A). Xenograft model mice were administered PBS, IgG-DX8951 (5 mg/kg), or EPI (7.5 mg/kg) as controls. DDR1-DX8951 induced remarkable and sustained tumor growth inhibition in all treated mice (Figs. 5B and C). The antitumor activities of DDR1-DX8951 were evaluated as the tumor mass decreased; the tumors in the treated group demonstrated a 94.7% greater reduction than those in the PBS group (Fig. 5D). In comparison, the EPI and IgG-DX8951 regimens had moderate efficacy against E0771 tumors and were significantly less effective than the DDR1-DX8951 regimen. These results are most likely attributable to the lack of DDR1 targetability. There was no significant difference in body weight among all groups (Fig. 5E). We further explored how DDR1-DX8951 elicits antitumor activity by measuring the TUNEL staining intensity and the $CD8^+$ and $CD4^+$ T-cell populations. TUNEL staining increased in the DDR1-DX8951 group compared with that in the other groups (Fig. 5F). Compared with those in the other groups, the $CD8^+$ and $CD4^+$ T-cell populations in the DDR1-DX8951 subgroup were also improved (Fig. 5F).

Subsequently, to confirm the optimum dosage of DDR1-DX8951, the antitumor activity of DDR1-DX8951 was reassessed using an ascending dosage (1, 5, or 10 mg/kg) in TNBC model mice (E0771) administered through the tail vein (Fig. 5G). The tumor inhibition rates of DDR1-DX8951 at 1, 5, and 10 mg/kg were 51.6%, 93.6%, and 98.4% higher, respectively, than those in the PBS group (Figs. 5H–J). The results demonstrated that 5 mg/kg DDR1-DX8951 can remarkably inhibit TNBC tumor growth sustainably. Therefore, 5 mg/kg was considered as the optimum DDR1-DX8951 concentration for targeted therapy for TNBC in preclinical mouse models.

The *in vivo* toxicity of DDR1-DX8951 was also evaluated at 1, 5, and 10 mg/kg doses by serum analysis. No significant change in mouse weight was observed among the different dosage groups (Fig. 5K). At the end of the investigation, mouse blood samples were analyzed to estimate AST and ALT levels. No DDR1-DX8951-treated mice demonstrated an increase in AST or ALT levels compared with those in the PBS group (Figs. 5L and M). Additionally, the renal toxicity of DDR1-DX8951 was assessed by analyzing the variations in Cre and BUN levels, and no renal toxicity was detected in the three dosage groups (Figs. 5N and O).

Fig. 5. Antitumor activity of discoidin domain receptor 1 (DDR1)-DX8951 in murine triple-negative breast cancer (TNBC) tumors *in vivo*. (A) Schematic design of *in vivo* efficacy of DDR1-DX8951 in the settings of an orthotopic TNBC model. (B) Image of excised orthotopic E0771 tumors from mice treated with phosphate-buffered solution (PBS), epirubicin (EPI), IgG-DX8951, or DDR1-DX8951 ($n = 5$). (C) Tumor progression was monitored by tumor volume measurement using a caliper. (D) Tumor mass at the end point (day 21) was quantified by weight. (E) Mouse body weights receiving PBS, EPI, IgG-DX8951, or DDR1-DX8951. (F) Representative images for hematoxylin and eosin (H&E), terminal deoxynucleotidyl transferase-dUTP nick end labeling (TUNEL) staining, and immune fluorescent double staining of T cell ($CD4^+$ and $CD8^+$) of the excised tumors. (G) Schematic design of dosage-dependent efficacy of DDR1-DX8951 in an orthotopic TNBC tumor model. (H) Image of excised orthotopic E0771 tumors from mice treated with PBS or DDR1-DX8951 at three different dosages. (I) Tumor progression receiving PBS or DDR1-DX8951 at different dosages was monitored by tumor volume. (J) Tumor mass at the end point (day 21) was quantified by weight. (K) Quantified mouse body weights during receiving DDR1-DX8951 at different dosages. (L–O) Chronic liver and renal toxicities of DDR1-DX8951 were analyzed by blood chemistry: quantitative analyses of alanine aminotransferase (ALT) (L), aspartate aminotransferase (AST) (M), creatinine (Cre) (N), and blood urea nitrogen (BUN) (O). *** $P < 0.001$. ADC: antibody-drug conjugates.



3.7. *In vivo* antitumor efficacy of DDR1-DX8951 plus pembrolizumab

We next evaluated the antitumor effects of DDR1-DX8951 on orthotopic TNBC tumor growth *in vivo* (Fig. 6A). DDR1-DX8951 or DDR1 antibody was intravenously administered to MDA-MB-231 tumor-bearing mice at 5 mg/kg per week. In comparison, as a control, pembrolizumab was intraperitoneally administered at dosages of 2.5 mg/kg on days 1, 4, 8, and 15. After two cycles of injection, compared with those in the other groups, DDR1-DX8951 plus pembrolizumab treatment resulted in remarkable and sustainable antitumor activity (Figs. 6B and C). The quantified tumor mass data demonstrated that compared with the PBS group, the DDR1-DX8951 plus pembrolizumab group had reduced TNBC tumor growth (Figs. 6D and E). The most obvious changes in apoptosis and necrosis were explored in the DDR1-DX8951 plus pembrolizumab group (Fig. 6F). Additionally, we explored the antitumor mechanism of DDR1-DX8951 plus pembrolizumab by analyzing DDR1 or Ki67 expression in TNBC tissue sections. The number of DDR1 or Ki67-positive cells in the DDR1-DX8951 plus pembrolizumab group was markedly lower than that in the other groups (Figs. 6G and H), resulting in marked and sustainable tumor growth inhibition. Moreover, the expression levels of CD31 were lower in the DDR1-DX8951 plus pembrolizumab group than in the other groups (Fig. 6I), as were TUNEL staining (Fig. 6J) and the proportions of CD8⁺ T cells (Figs. 6K and L).

Subsequently, we explored the antitumor immune responses elicited through this synergistic treatment to further determine the mechanism underlying the potent antitumor activities of DDR1-DX8951 plus pembrolizumab. The percentage of CD8⁺ T cells (CD45⁺CD3⁺CD8⁺) in the tumor tissue was examined via flow cytometry. The percentage of tumor-infiltrated CD8⁺ T cells increased from 3.51% ± 0.2% in the PBS group to 10.2% ± 0.8% in the DDR1-DX8951 group (Fig. 6M), likely due to the promotion of CD8⁺ T-cell migration by the DDR1 antibody-mediated collagen fibre rearrangement. In contrast, the percentage of tumor-infiltrated CD8⁺ T cells increased to 22.1% ± 1.8% in the DDR1-DX8951 plus pembrolizumab group, verifying that the pembrolizumab-mediated blockade of the inhibitory PD-1 and PD-L1 signaling pathways and collagen fibre rearrangement in the extracellular matrix ultimately facilitated the infiltration of CD8⁺ T cells. The IF results coincided with the flow cytometry results, where conspicuous red fluorescence was observed in the DDR1-DX8951 plus pembrolizumab group. Additionally, the DDR1-DX8951 plus pembrolizumab combination elevated the serum levels of tumor-suppressing cytokines, such as TNF- α (Fig. 6N), IL-2 (Fig. 6O), and IFN- γ (Fig. 6P), to a greater extent than those observed in the other groups. These findings demonstrate that combination treatment with DDR1-DX8951 and pembrolizumab can trigger antitumor immune responses and significantly improve immune efficacy.

3.8. *In vivo* antimetastatic efficacy of DDR1-DX8951 plus pembrolizumab

Given that DDR1-DX8951 and pembrolizumab induced potent systemic immune responses, we subsequently evaluated the

antimetastatic efficacy of DDR1-DX8951 and pembrolizumab. Metastatic tumor-bearing mice administered different formulations were sacrificed for analysis (Fig. 7A). Lungs and livers were collected, stained with H&E, and imaged to count the pulmonary and liver metastatic nodules. The imaging and quantification data (Figs. 7B–E) demonstrated a remarkable reduction in pulmonary metastasis (3-fold) and liver metastasis (9-fold), revealing the potent antimetastatic efficacy of DDR1-DX8951 treatment versus the PBS control. Furthermore, notably, liver and pulmonary metastatic nodules were rarely observed in the DDR1-DX8951 and pembrolizumab groups (3.7- and 2-fold less common than in the DDR1-DX8951 group, respectively). H&E staining also verified that the DDR1-DX8951 and pembrolizumab groups had the fewest metastatic nodules (Fig. 7C). Therefore, the above results confirmed that the introduction of DDR1-DX8951 and pembrolizumab could decrease pulmonary and liver metastasis via the synergistic effect of DDR1-DX8951 and pembrolizumab (Figs. 7D and E). Additionally, in comparison to those in the PBS group, DDR1-DX8951 and pembrolizumab treatment significantly extended the survival time of the mice (Fig. 7F), indicating the potent antimetastatic efficacy of the combination therapy of DDR1-DX8951 and pembrolizumab in the treatment of TNBC.

4. Discussion

We constructed a targeted and effective ADC, DDR1-DX8951, and combined it with immune checkpoint inhibitors, revealing a novel and promising strategy for TNBC-targeted therapy. The results indicated that specific drugs can be delivered to TNBC cells through cell membrane DDR1 receptor mediation by coupling DDR1 antibodies and small-molecule cytotoxic drugs; this targeting reduces the accumulation of the drug in normal tissue, potentially substantially reducing off-target effects. Furthermore, the DDR1 antibody disrupted extracellular collagen fibre alignment and promoted T-cell infiltration; thus, DDR1-DX8951 plus pembrolizumab may improve TNBC treatment. TNBC tumors in xenograft mouse models can be effectively inhibited by DDR1-DX8951 plus pembrolizumab, contributing to remarkable growth suppression of tumor and metastasis. Our novel strategy depends on DDR1, the promising target for TNBC identified through quantitative screening. In addition, the introduction of pembrolizumab provides a novel immunotherapy approach for evaluating the synergistic therapeutic effect of DDR1-DX8951 plus pembrolizumab in TNBC tumors.

Our data provide evidence that DDR1-DX8951 plus pembrolizumab is a targeted and synergistic immune therapy approach for TNBC. Many strategies have been found to enhance therapeutic effects primarily confined by dose-dependent cytotoxicity. However, these agents, such as liposomal and albumin-bound cytotoxic formulations, are rarely authorized for use in clinical practice. Compared with liposomal or albumin formulations with a diameter of 100 nm, ADCs have a substantial advantage in terms of size (approximately 10 nm) and can escape from phagocytosis by the reticular endothelial system, resulting in prolonged circulation in the peripheral blood [42]. The blood half-life of ADCs is approximately 100 h, unlike that of albumin or liposomal formulations

Fig. 6. Antitumor activity of discoidin domain receptor 1 (DDR1)-DX8951 in human triple-negative breast cancer (TNBC) tumors *in vivo*. (A) Schematic diagram of an orthotopic TNBC model injected MDA-MB-231 at day 0, receiving phosphate-buffered solution (PBS) + peripheral blood mononuclear cell (PBMC), pembrolizumab + PBMC, DDR1 + PBMC, DDR1-DX8951 + PBMC, or DDR1-DX8951 + pembrolizumab + PBMC at different time points post tumor inoculation ($n = 5$). (B) The size of dissected tumor tissues. (C) Tumor progression was monitored by tumor volume measurement using a caliper. (D) The tumor sizes in each group. (E) The tumor weight in each group. (F) Tumor sections were stained with hematoxylin and eosin (H&E), DDR1, Ki67, CD31, terminal deoxynucleotidyl transferase-dUTP nick end labeling (TUNEL), and immunofluorescent double staining of T cell (CD4⁺ and CD8⁺) for histological analyses. (G–K) Quantitative analyses of DDR1 (G), Ki67 (H), CD31 (I), TUNEL (J), and immunofluorescent double staining of T cell (CD4⁺ and CD8⁺) (K) in tumors of different treatment groups. (L) Representative flow cytometry plots. (M) Quantitative analysis data of CD8⁺ T in tumors ($n = 5$). (N–P) Cytokine concentrations of tumor necrosis factor- α (TNF- α) (N), interleukin 2 (IL-2) (O), and interferon- γ (INF- γ) (P) in serum ($n = 5$). * $P < 0.05$, ** $P < 0.01$, and *** $P < 0.001$.

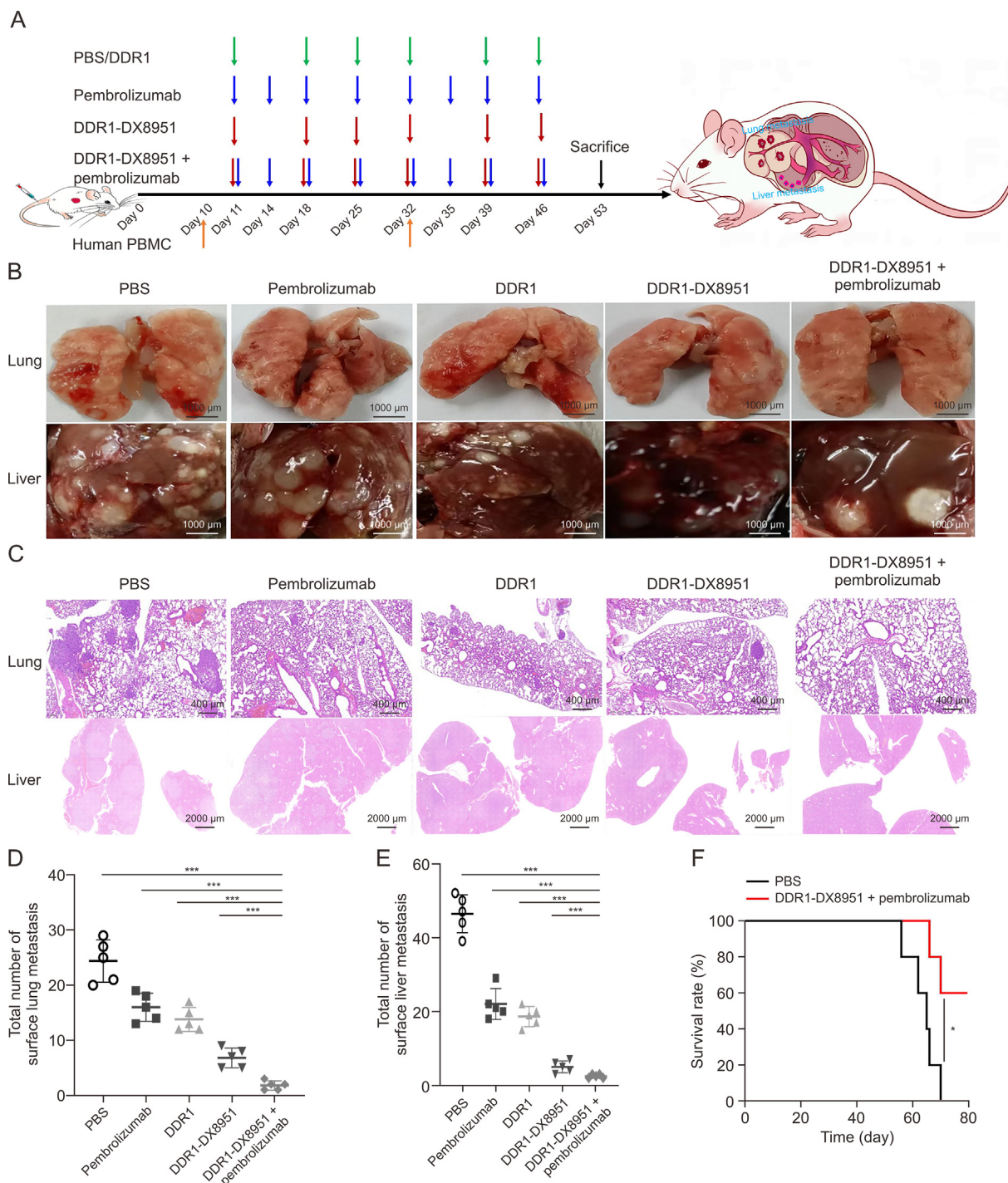


Fig. 7. *In vivo* antimetastasis effect of discoidin domain receptor 1 (DDR1)-DX8951 + pembrolizumab. (A) Schematic indicative of antimetastasis assessment. (B) Representative images of the lungs and livers excised from various treated mice. (C) Representative images from the hematoxylin and eosin (H&E) assays of lungs and livers. (D, E) Numbers of metastatic lung (D) and liver (E) modules were quantified for mice in the indicated treatment groups. (F) Survival curves of different treated mice ($n = 5$). * $P < 0.05$ and *** $P < 0.001$. PBS: phosphate-buffered solution; PBMC: peripheral blood mononuclear cell.

(20–30 h) [43]. The advantages of active targeting and an extended half-life will be instrumental in achieving more efficient aggregation in the tumor mass and reduced distribution to major organs. In contrast, nab-paclitaxel, a representative albumin-bound cytotoxic drug approved for TNBC treatment, easily dissociates during blood circulation due to the limited adhesion between paclitaxel and albumin, contributing to severe peripheral neurotoxicity and unsatisfactory efficacy [42]. Metronomic administration methods can

improve therapeutic efficacy [44], for example, by adjusting the dosing frequency. However, no specific target exists for these formulations. Our novel concept of conjugating small-molecule cytotoxic drugs to a targeting antibody can dramatically increase the efficiency of these targeted drugs [45].

Our findings indicate that DDR1-ADC effectively targets TNBC, given its increased expression and desired cell internalization. Because DS-8201a, an ADC that has been authorized to overcome

various types of tumors [46,47], has demonstrated surprising efficacy in treating human epidermal growth factor receptor 2-positive breast cancer, enhancing progression-free survival by 25.1 months [48,49], multiple clinical trials of ADC drugs are being conducted on breast cancer patients [50]. Nevertheless, few of the ADC targets for TNBC have demonstrated significant therapeutic efficacy or mild toxicity. In contrast, DDR1 protein is expressed at comparatively greater levels in TNBC cells than in epidermal growth factor receptor (EGFR) (approximately 3.5-fold greater than that in the controls), while the expression level of EGFR is approximately equivalent to that in the controls. The comparatively higher expression levels of DDR1 in TNBC cells may make it an ideal and effective therapeutic target. One unique ADC for TNBC that has been officially sanctioned is sacituzumab govitecan [5]. Although sacituzumab govitecan has been shown to prolong survival, only some patients can benefit from this ADC therapy because it causes severe neutropenia and diarrhea [51]. Recently, DDR1 was found to be an ideal target in targeted therapy for colon tumors, confirming the precise targeting of DDR1 with decreased agglomeration in major organs [52]. Importantly, as demonstrated in our investigations, DDR1-DX8951 significantly suppressed TNBC cell proliferation *in vitro* and exerted greater antitumor effects *in vivo* than the control treatment. Furthermore, *in vivo*, liver and kidney toxicity were not detected after DDR1-DX8951 treatment at a dose of 5 mg/kg. Nevertheless, animal studies with larger treatment groups are necessary for long-term safety determination before proceeding to clinical trials in humans.

Previous research has demonstrated that DDR1 impedes the penetration of CD8⁺ T cells into tumors, restricting T cells to the tumor margin area. The high affinity of DDR1 antibodies for DDR1 receptors results in collagen fibre rearrangement, promoting immune cell penetration and mitigating immune exclusion. In a xenograft model of TNBC, the introduction of DDR1 antibodies elicited complete tumor regression, providing encouraging proof-of-principle evidence for antitumor activity. These inspiring discoveries prompted us to investigate the use of DDR1 antibodies combined with other immunotherapies, such as immune checkpoint inhibitors. DDR1-DX8951 plus pembrolizumab had a synergistic antitumor effect in this preclinical TNBC study. Although there could be an unavoidable disparity between animal models and patients when translating these findings into clinical practice, DDR1-DX8951 plus pembrolizumab is a promising potential therapeutic strategy with synergistic antitumor efficacy resulting from the combination of the ADC and immunotherapeutic. The combination of DDR1-DX8951 and pembrolizumab had a stronger antitumor effect than either drug alone. The possible mechanisms are as follows: 1) the targeted accumulation and release of the small-molecule DX8951, 2) collagen fibre rearrangement allowing CD8⁺ T-cell migration, and 3) blocking of the damaging PD-1/PD-L1 pathway by pembrolizumab, improving the response of CD8⁺ T cells and enhancing the efficacy of DDR1-DX8951. The outcomes of this investigation demonstrated promising preclinical evidence for the use of DDR1-DX8951 combined with immune checkpoint inhibitors. Further research and clinical trials are required to confirm the efficacy of this combination treatment in various tumor types.

5. Conclusions

The preliminary results presented here provide preclinical evidence that DDR1-DX8951 in combination with pembrolizumab could be an effective TNBC therapy, encouraging clinical translational research in DDR1-overexpressing TNBC tumors. This investigation also provides evidence for the need for additional large-sample studies to further assess the safety and efficacy of DDR1-DX8951 plus pembrolizumab in clinical trials. Furthermore,

this combination therapy strategy incorporating immune checkpoint inhibitors could be used for the synergistic therapy of TNBC and other DDR1-overexpressing solid tumors. This approach could be used in additional clinical trials focused on tumor targeting and immunotherapy.

CRedit authorship contribution statement

Shoubing Zhou: Writing – review & editing, Writing – original draft, Visualization, Validation, Data curation. **Wenyu Li:** Writing – original draft, Methodology, Investigation, Formal analysis. **Dan Zhao:** Methodology, Investigation, Formal analysis. **Qiujuan Zhang:** Methodology, Investigation. **Hu Liu:** Validation, Resources, Methodology. **Tengchuan Jin:** Writing – review & editing, Resources, Data curation, Conceptualization. **Yueyin Pan:** Supervision, Resources, Project administration, Conceptualization.

Declaration of competing interest

The authors declare that there are no conflicts of interest.

Acknowledgments

This work was supported by Anhui Province Clinical Key Specialty Construction Project, China (Grant No.: 2021sjlczdzk), the National Key Research and Development Program of China (Grants Nos.: 2022YFC2304102 and 2022YFC2303300), and the National Natural Science Foundation of China (Grant Nos.: 82272301, 32100745, and 31971129).

Appendix A. Supplementary data

Supplementary data to this article can be found online at <https://doi.org/10.1016/j.jpha.2024.101100>.

References

- [1] C. Frankenberger, D. Rabe, R. Bainer, et al., Metastasis suppressors regulate the tumor microenvironment by blocking recruitment of prometastatic tumor-associated macrophages, *Cancer Res.* 75 (2015) 4063–4073.
- [2] E. Choupani, M. Mahmoudi Gomari, S. Zanganeh, et al., Newly developed targeted therapies against the androgen receptor in triple-negative breast cancer: A review, *Pharmacol. Rev.* 75 (2023) 309–327.
- [3] F. Batalini, D.C. Gulhan, V. Mao, et al., Mutational signature 3 detected from clinical panel sequencing is associated with responses to olaparib in breast and ovarian cancers, *Clin. Cancer Res.* 28 (2022) 4714–4723.
- [4] M.A.C. Bruin, G.S. Sonke, J.H. Beijnen, et al., Pharmacokinetics and pharmacodynamics of PARP inhibitors in oncology, *Clin. Pharmacokinet.* 61 (2022) 1649–1675.
- [5] A. Bardia, S.A. Hurvitz, S.M. Tolaney, et al., Sacituzumab govitecan in metastatic triple-negative breast cancer, *N. Engl. J. Med.* 384 (2021) 1529–1541.
- [6] X. Zhong, W. Zhang, T. Sun, DDR1 promotes breast tumor growth by suppressing antitumor immunity, *Oncol. Rep.* 42 (2019) 2844–2854.
- [7] X. Sun, B. Wu, H.C. Chiang, et al., Tumour DDR1 promotes collagen fibre alignment to instigate immune exclusion, *Nature* 599 (2021) 673–678.
- [8] D.L. Wagner, E. Klotzsch, Barring the gates to the battleground: DDR1 promotes immune exclusion in solid tumors, *Signal Transduct. Target. Ther.* 7 (2022), 17.
- [9] J. Jacob, L.E. Francisco, T. Chatterjee, et al., An antibody-drug conjugate targeting GPR56 demonstrates efficacy in preclinical models of colorectal cancer, *Br. J. Cancer* 128 (2023) 1592–1602.
- [10] J. Zhang, R. Liu, S. Gao, et al., Phase I study of A166, an antibody–drug conjugate in advanced HER2-expressing solid tumours, *NPJ Breast Cancer* 9 (2023), 28.
- [11] Z. Najminejad, F. Dehghani, Y. Mirzaei, et al., Clinical perspective: Antibody-drug conjugates for the treatment of HER2-positive breast cancer, *Mol. Ther.* 31 (2023) 1874–1903.
- [12] Y.A. Heo, Mirvetuximab soravtansine: First approval, *Drugs* 83 (2023) 265–273.
- [13] M.S.J. McDermott, N.A. O'Brien, B. Hoffstrom, et al., Preclinical efficacy of the antibody-drug conjugate CLDN6-23-ADC for the treatment of CLDN6-positive solid tumors, *Clin. Cancer Res.* 29 (2023) 2131–2143.
- [14] R.J. Evans, D.W. Perkins, J. Selve, et al., Endo180 (MRC2) antibody-drug conjugate for the treatment of sarcoma, *Mol. Cancer Ther.* 22 (2023) 240–253.

- [15] N. Coleman, T.A. Yap, J.V. Heymach, et al., Antibody-drug conjugates in lung cancer: Dawn of a new era? *NPJ Precis. Oncol.* 7 (2023), 5.
- [16] W. Weng, T. Meng, Q. Zhao, et al., Antibody-exatecan conjugates with a novel self-immolative moiety overcome resistance in colon and lung cancer, *Cancer Discov.* 13 (2023) 950–973.
- [17] A. Tolcher, E. Hamilton, R.L. Coleman, The evolving landscape of antibody-drug conjugates in gynecologic cancers, *Cancer Treat. Rev.* 116 (2023), 102546.
- [18] J. Bi, Z. Wu, X. Zhang, et al., TMEM25 inhibits monomeric EGFR-mediated STAT3 activation in basal state to suppress triple-negative breast cancer progression, *Nat. Commun.* 14 (2023), 2342.
- [19] R. Taftaf, X. Liu, S. Singh, et al., ICAM1 initiates CTC cluster formation and trans-endothelial migration in lung metastasis of breast cancer, *Nat. Commun.* 12 (2021), 4867.
- [20] M.E. Silva, M. Hernández-Andrade, N. Abasolo, et al., DDR1 and its ligand, collagen IV, are involved in *in vitro* oligodendrocyte maturation, *Int. J. Mol. Sci.* 24 (2023), 1742.
- [21] L. Zhang, N. Lou, Q. Yu, et al., Association of DDR1 with immune exclusion and outcomes in non-small cell lung cancer, *J. Clin. Oncol.* 40 (2022), e20553.
- [22] H. Su, F. Yang, R. Fu, et al., Collagenolysis-dependent DDR1 signalling dictates pancreatic cancer outcome, *Nature* 610 (2022) 366–372.
- [23] X. Duan, X. Xu, Y. Zhang, et al., DDR1 functions as an immune negative factor in colorectal cancer by regulating tumor-infiltrating T cells through IL-18, *Cancer Sci.* 113 (2022) 3672–3685.
- [24] Y. Xiong, X. Zhang, J. Zhu, et al., Collagen I-DDR1 signaling promotes hepatocellular carcinoma cell stemness via Hippo signaling repression, *Cell Death Differ* 30 (2023) 1648–1665.
- [25] D. Jiang, X. Gao, R. Tan, et al., Euphorbia factor L1 suppresses breast cancer liver metastasis via DDR1-mediated immune infiltration, *Aging* 15 (2023) 9217–9229.
- [26] A.Y. Wang, N.M. Coelho, P.D. Arora, et al., DDR1 associates with TRPV4 in cell-matrix adhesions to enable calcium-regulated myosin activity and collagen compaction, *J. Cell. Physiol.* 237 (2022) 2451–2468.
- [27] Y. Tian, F. Bai, D. Zhang, New target DDR1: A “double-edged sword” in solid tumors, *Biochim. Biophys. Acta Rev. Cancer* 1878 (2023), 188829.
- [28] J. Liu, H.C. Chiang, W. Xiong, et al., A highly selective humanized DDR1 MAb reverses immune exclusion by disrupting collagen fiber alignment in breast cancer, *J. Immunother. Cancer* 11 (2023), e006720.
- [29] ClinicalTrials.gov, A first-in-human study of PRTH-101 monotherapy +/- pembrolizumab in subjects with advanced malignancies. <https://clinicaltrials.gov/study/NCT05753722>. (Accessed 5 June 2024).
- [30] N. Vey, F.J. Giles, H. Kantarjian, et al., The topoisomerase I inhibitor DX-8951f is active in a severe combined immunodeficient mouse model of human acute myelogenous leukemia, *Clin. Cancer Res.* 6 (2000) 731–736.
- [31] S. Sharma, N. Kemeny, G.K. Schwartz, et al., Phase I study of topoisomerase I inhibitor exatecan mesylate (DX-8951f) given as weekly 24-hour infusions three of every four weeks, *Clin. Cancer Res.* 7 (2001) 3963–3970.
- [32] Q. Tang, S. Li, G. Huang, et al., Research progress on PD-1 and PD-L1 inhibitors in the treatment of metastatic urothelial carcinoma, *Int. Immunopharmacol.* 119 (2023), 110158.
- [33] T. Wei, K. Wang, S. Liu, et al., Periostin deficiency reduces PD-1+ tumor-associated macrophage infiltration and enhances anti-PD-1 efficacy in colorectal cancer, *Cell Rep* 42 (2023), 112090.
- [34] Q. Huang, X. Wu, Z. Wang, et al., The primordial differentiation of tumor-specific memory CD8+ T cells as bona fide responders to PD-1/PD-L1 blockade in draining lymph nodes, *Cell* 185 (2022) 4049–4066.e25.
- [35] J. Cortes, H.S. Rugo, D.W. Cescon, et al., Pembrolizumab plus chemotherapy in advanced triple-negative breast cancer, *N. Engl. J. Med.* 387 (2022) 217–226.
- [36] P. Guo, J. Yang, D. Liu, et al., Dual complementary liposomes inhibit triple-negative breast tumor progression and metastasis, *Sci. Adv.* 5 (2019), eaav5010.
- [37] X. Shen, S. Xie, X. Zheng, et al., Cirrhotic-extracellular matrix attenuates aPD-1 treatment response by initiating immunosuppressive neutrophil extracellular traps formation in hepatocellular carcinoma, *Exp. Hematol. Oncol.* 13 (2024), 20.
- [38] J. Huang, A.T. Agoston, P. Guo, et al., A rationally designed ICAM1 antibody drug conjugate for pancreatic cancer, *Adv. Sci. (Weinh.)* 7 (2020), 2002852.
- [39] S.R. Adams, H.C. Yang, E.N. Savariar, et al., Anti-tubulin drugs conjugated to anti-ErbB antibodies selectively radiosensitize, *Nat. Commun.* 7 (2016), 13019.
- [40] A. Costales-Carrera, A. Fernández-Barral, P. Bustamante-Madrid, et al., Plocabulin displays strong cytotoxic activity in a personalized colon cancer patient-derived 3D organoid assay, *Mar. Drugs* 17 (2019), 648.
- [41] Y. Wu, Q. Li, Y. Kong, et al., A highly stable human single-domain antibody-drug conjugate exhibits superior penetration and treatment of solid tumors, *Mol. Ther.* 30 (2022) 2785–2799.
- [42] O. Borgå, E. Lilienberg, H. Bjeremo, et al., Pharmacokinetics of total and unbound paclitaxel after administration of paclitaxel micellar or nab-paclitaxel: An open, randomized, cross-over, explorative study in breast cancer patients, *Adv. Ther.* 36 (2019) 2825–2837.
- [43] S. Girish, M. Gupta, B. Wang, et al., Clinical pharmacology of trastuzumab emtansine (T-DM1): An antibody-drug conjugate in development for the treatment of HER2-positive cancer, *Cancer Chemother. Pharmacol.* 69 (2012) 1229–1240.
- [44] R.A. Previs, G.N. Armaiz-Pena, Y.G. Lin, et al., Dual metronomic chemotherapy with nab-paclitaxel and topotecan has potent antiangiogenic activity in ovarian cancer, *Mol. Cancer Ther.* 14 (2015) 2677–2686.
- [45] W. Cao, H. Xing, Y. Li, et al., Claudin18.2 is a novel molecular biomarker for tumor-targeted immunotherapy, *Biomark. Res.* 10 (2022), 38.
- [46] T. Yoshino, M. Di Bartolomeo, K. Raghav, et al., Final results of DESTINY-CRC01 investigating trastuzumab deruxtecan in patients with HER2-expressing metastatic colorectal cancer, *Nat. Commun.* 14 (2023), 3332.
- [47] E. Van Cutsem, M. di Bartolomeo, E. Smyth, et al., Trastuzumab deruxtecan in patients in the USA and Europe with HER2-positive advanced gastric or gastroesophageal junction cancer with disease progression on or after a trastuzumab-containing regimen (DESTINY-Gastric02): Primary and updated analyses from a single-arm, phase 2 study, *Lancet Oncol.* 24 (2023) 744–756.
- [48] J. Cortés, S.B. Kim, W.P. Chung, et al., LBA1 Trastuzumab deruxtecan (T-DXd) vs trastuzumab emtansine (T-DM1) in patients (Pts) with HER2+ metastatic breast cancer (mBC): Results of the randomized phase III DESTINY-Breast03 study, *Ann. Oncol.* 32 (2021) S1287–S1288.
- [49] E.P. Hamilton, V.P.H. Bragaia, W. Yeo, et al., Trastuzumab deruxtecan (T-DXd) versus trastuzumab emtansine (T-DM1) in patients (pts) with HER2-positive (HER2+) unresectable and/or metastatic breast cancer (mBC): Safety follow-up of the randomized, phase 3 study DESTINY-Breast03, *J. Clin. Oncol.* 40 (2022), 1000.
- [50] M.A. Subhan, V.P. Torchilin, Advances in targeted therapy of breast cancer with antibody-drug conjugate, *Pharmaceutics* 15 (2023), 1242.
- [51] A.R. Schreiber, M. Andress, J.R. Diamond, Tackling metastatic triple-negative breast cancer with sacituzumab govitecan, *Expert Rev. Anticancer Ther.* 21 (2021) 1303–1311.
- [52] Y. Tao, R. Wang, Q. Lai, et al., Targeting of DDR1 with antibody-drug conjugates has antitumor effects in a mouse model of colon carcinoma, *Mol. Oncol.* 13 (2019) 1855–1873.